# FIRST VLA OBSERVATIONS OF NONTHERMAL METRIC BURSTS ASSOCIATED WITH CORONAL MASS EJECTIONS DETECTED BY THE *SOLAR AND HELIOSPHERIC OBSERVATORY*

R. F. WILLSON, S. L. REDFIELD, AND K. R. LANG

Department of Physics and Astronomy, Tufts University, Medford, MA 02155

B. J. THOMPSON

*SOHO* Experiment Operations and Analysis Facility, NASA/Goddard Space Flight Center, Greenbelt, MD 20771

AND

O. C. ST. CYR

CPI/Naval Research Laboratory, Code 682.3, NASA/Goddard Space Flight Center, Greenbelt, MD 20771

## ABSTRACT

We present the first observations of nonthermal decimetric burst emission of the Sun using the new 400 cm (74 MHz) system at the VLA. Our VLA observations were carried out in collaboration with the Large Angle Spectroscopic Coronagraph (LASCO) and the Extreme-Ultraviolet Imaging Telescope (EIT) on board the *Solar and Heliospheric Observatory* spacecraft. Full-disk observations at 400 and 91 cm were used to study the spatial and temporal variations of nonthermal radio bursts during coronal mass ejections (CMEs) detected by LASCO as well as transient extreme-ultraviolet brightenings detected by the EIT. VLA snapshot maps at 400 cm revealed impulsive burst emission in the low corona that began near the estimated start time of the CME activity; that beginning also coincided with a C1.1 GOES X-ray burst and an EIT flarelike brightening. The nonthermal metric bursts then continued sporadically during the next several hours, which included the ejection of spatially separated CME components. The 400 cm bursts are contained within curved, or archlike, sources at a fixed radial distance but with a varying position between two active regions detected by the EIT near the limb, suggesting that they were emitted within large-scale magnetic loops. Our 91 cm observations also show the onset of a long-lasting type I noise storm following the initiation of CME activity, again suggesting an intimate relationship between the production of nonthermal particles and large-scale evolving plasma–magnetic field structures in the corona.

*Subject headings:* Sun: corona — Sun: radio radiation

## 1. INTRODUCTION

High-resolution Very Large Array (VLA) observations of the Sun at 91 cm wavelength have provided new information about the properties of long-lasting, nonthermal type I noise storms, showing that these sources are often located along large-scale magnetic loops that link widely separated active regions on the solar surface (White, Thejappa, & Kundu 1992; Willson et al. 1995; Bogod et al. 1995; Krucker et al. 1995; Willson, Kile, & Rothberg 1997).

We now have the opportunity to extend these investigations to a considerably longer wavelength by using the recently installed 74 MHz (400 cm) system at the VLA. Observations at 400 cm are of particular interest because they have the potential to detect the metric signatures of nonthermal processes associated with solar transient events such as flares and coronal mass ejections (CMEs). Metric radio bursts, such as types II and III bursts, are, for example, respectively produced by shock waves and energetic particles that can be associated with CMEs (Wagner 1984). The radio bursts provide information on the nonthermal electrons, the magnetic field strength, and sometimes the coronal structure of the magnetic fields involved (Trottet et al. 1982).

Other than the pioneering detection with the Culgoora radioheliograph at 80 MHz (Sheridan et al. 1978), we are aware of only two reports of radio imaging of CMEs (Gopalswamy & Kundu 1992, 1993; Pick et al. 1997, 1998). In both cases, type III bursts were detected during the formation and initial acceleration of the CME. The 400 cm images obtained by Gopalswamy & Kundu (1993) with the now-defunct Clark Lake instrument indicated that the meter-wavelength source was confined radially into a large loop or arcade structure at

a level where the plasma frequency corresponds to the observed frequency. The images obtained by Pick et al. (1997, 1998) with the Nancay Radioheliograph at higher frequencies (164, 236, 327, and 444 MHz) were spatially associated with the CME detected by the Large Angle Spectrospcopic Coronagraph (LASCO) on board the *Solar and Heliospheric Observatory* (*SOHO*).

Here we report the first observations of nonthermal decimetric burst emission using the new 400 cm (74 MHz) system at the VLA, demonstrating its remarkable capacity for high resolution in space (30″) and time (10 s). Our VLA observations were carried out in collaboration with *SOHO*; the LASCO C2 coronagraph was used to obtain white-light images of CME activity, while *SOHO*'s Extreme-Ultraviolet Imaging Telescope (EIT) was used to detect the $10^6$ K plasma in active regions and solar flares that might initiate CMEs. Full-disk VLA observations at 400 and 91 cm were used to study the spatial and temporal variations of nonthermal radio bursts during the CME-related activity detected by LASCO, the EIT, and the Mauna Loa Mark-III coronagraph. VLA snapshot maps at 400 cm revealed impulsive burst emission in the low corona that began near the estimated start time of the CME activity. The nonthermal metric bursts continued sporadically during the next several hours, which included the ejection of spatially separated CME components. The 400 cm bursts are contained within curved or archlike sources at a fixed radial distance but with a varying position between two active regions near the limb, which suggests that they were emitted within large-scale magnetic loops. Our 91 cm observations also show the onset of a type I noise storm following the initiation of CME activity, again suggesting an intimate relationship between the produc-
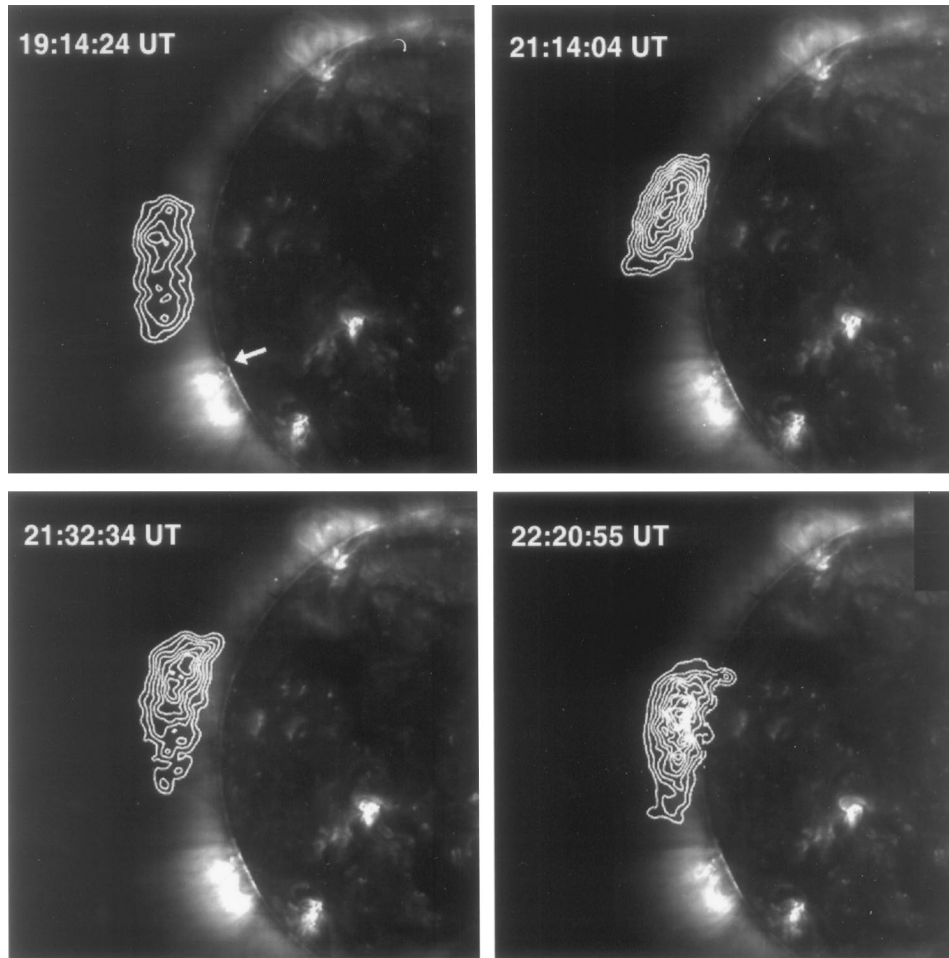
FIG. 1.—VLA snapshot maps of intense nonthermal activity at 400 cm wavelength taken in 10 s intervals on 1998 March 8 at the times indicated. They are superposed on *SOHO* EIT images taken in the 195 Å line of Fe XII, formed at $1.5 \times 10^6$ K, within a few minutes of the VLA snapshot maps. The field of view is $30' \times 30'$. The contours denote levels of equal brightness temperature $T_b$ corresponding to $T_b = 1, 2, 3, ..., 10 \times 10^6$ K at 19:14:24 UT and 21:14:04 UT, $T_b = 5, 10, 15, ..., 35 \times 10^6$ K at 21:32:34 UT, and $T_b = 10, 20, 30, ..., 90 \times 10^6$ K at 22:20:55 UT. The arrow on the image taken at 19:14:24 UT shows the location of an EUV brightening detected on the EIT image 10 s earlier. The 400 cm radiation remains at the same radial distance from the solar surface, probably denoting the level at which the plasma frequency is close to the observing frequency of 74 MHz, but the radio bursts appear to move along the archlike or looplike structure that probably describes otherwise invisible, large-scale magnetic fields in the corona. They may be linked to one of the active regions denoted by bright EIT features.

tion of nonthermal particles and large-scale plasma–magnetic field structures in the corona.

## 2. OBSERVATIONS

### 2.1. *VLA Observations*

The VLA was used to observe the full solar disk Sun at 400 cm (73.8 MHz) and 91.6 cm (327.5 MHz) between 1800 and 2230 UT on 1998 March 8 in coordination with the *SOHO* EIT and LASCO. The primary beamwidths of the antennas at 400 and 91.6 cm are $\approx 600'$ and $150'$, respectively, allowing a global perspective of thermal and nonthermal activity within and between active regions and out into the low and middle corona. At the time of these observations, the VLA was in the A configuration, which provided synthesized beamwidths of $5''$ at 91 cm and $35''$ at 400 cm. Our observations were made in the spectral line mode using a 64 channel autocorrelator with a total bandwidth of 1.625 MHz, allowing us to examine individual frequency channels and to remove any narrowband interference that might otherwise contaminate the data but limiting its sampling time to 10 s.

Our 400 cm observing sequence consisted of 2 minute ob-

servations of the Sun followed by 2 minute observations of the nearby calibrator source 3C 446. This relatively rapid cadence of calibrator observations allowed us to compensate for phase and amplitude errors caused by the changes in the ionospheric refraction at low radio frequencies (Stewart & McLean 1982; Erickson 1984). The flux of 3C 446 (31.6 Jy) was bootstrapped from observations of 3C 48, whose flux was taken to be 75.5 Jy at 74 MHz. Finally, because the Sun's total flux at 400 cm is comparable to that of nonsolar sources and does not saturate the VLA receivers as it does at other bands (T. Bastian 1998, private communication), the normal procedure of inserting attenuators before the solar signals reach the receiver front ends could not be used. This prevented us from obtaining data simultaneously at 400 and 91 cm, as can be done, for example, at 20 and 91 cm wavelengths.

The 91.6 cm observations were instead made separately during four 10 minute periods in the normal solar continuum mode (i.e., using solar attenuators) with a bandwidth of 3.25 MHz and a time resolution of 1.67 s. Prior to each solar observation, the amplitudes and phases at 91 cm were calibrated using 5 minute observations of the source 3C 48.
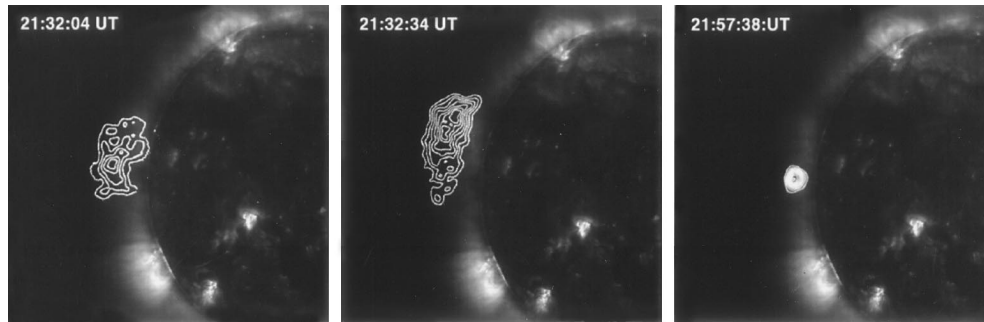
Fig. 2.—VLA snapshot maps at 400 cm (*left* and *center*) and 91.6 cm (*right*) wavelength taken in 10 s intervals on 1998 March 8 at the times indicated. They are superposed on *SOHO* EIT images taken in the 195 Å line of Fe XII, formed at $1.5 \times 10^6$ K, within a few minutes of the VLA snapshot maps. The field of view is $30' \times 30'$. The snapshot maps at 21:32:04 UT and 21:32:34 UT show 400 cm continuum and burst sources, respectively. Note that the 400 cm burst emission is displaced about $5'$ northward of the 400 cm continuum source. The image at 21:57:38 UT shows the location of a 91.6 cm type I noise storm source located southward and limbward of the 400 cm sources. The contours denote levels of equal brightness temperature $T_b$ corresponding to $T_b = 2, 4, 6, ..., 18 \times 10^5$ K at 21:32:04 and 21:57:38 UT and $T_b = 5, 10, 15, ..., 35 \times 10^6$ K at 21:32:34 UT.

## 2.2. *EIT and LASCO Observations*

The EIT was used to image a target active region, AR 8175 (N44°, E56°), in the coronal lines of Fe XII (195 Å), with a formation temperature of about $1.5 \times 10^6$ K over a field of view of $7' \times 7'$ every 4–6 minutes and to provide full-disk Fe XII images every 17 minutes. During the period of VLA observations, LASCO was operating in its CME patrol mode by producing C2 images (field of view from 2.0 to 6.0 $R_\odot$) every 30 minutes and C1 and C3 images more sporadically.

## 2.3. *Observational Results*

The calibrated 400 and 91.6 cm data sets were used to produce snapshot maps of total intensity $I$ and circular polarization $V$ at 10 s intervals throughout the 4.5 hr period of observation. In Figures 1 and 2, we compare VLA snapshot maps with EIT images of the Fe XII line (195 Å). The VLA images show both impulsive and slowly varying sources above the east limb at 91.6 and 400 cm. The VLA antennas are moved outward to their widest separation ($\approx 21$ km from the array center) in the A configuration, which overresolves the extended, low brightness temperature emission from the quiet Sun. Many of the longer baselines (length $\geq 5$ km) detect no correlated flux, but the shorter ones have detected and resolved the nonthermal burst sources associated with CMEs. The more extended thermal emission of CMEs detected with coronagraphs may be best observed in the more compact VLA configurations.

The 400 cm sources have half-intensity angular sizes of $\approx 2.5 \times 5'$ and lie at a nearly fixed radial height of $h \approx 0.3$ $R_\odot$ but with a varying position along an arc that appears to lie parallel to the solar limb. Time profiles at 400 cm reveal impulsive (duration $\Delta t \leq 10$ s) bursts with peak brightness temperatures as high as $T_b \approx 5 \times 10^7$ K superposed on a nearly constant emission level having a significantly lower brightness temperature of $T_b \approx 5 \times 10^5$ K. In general, the snapshot maps show that the peaks of the bursting sources lie a few arcminutes north of the fainter, more slowly varying sources, which suggests that these two components are produced by different emission mechanisms and under different excitation conditions. Neither the impulsive nor the slowly varying sources have any detectable circular polarization above a level of $\rho_c \leq 10\%$. Although it is impossible, in the absence of simultaneous dynamic spectral data, to unambiguously identify the specific type of burst that was observed, the high brightness temperature, short duration, and absence of circular polarization of the bursting

sources leads us to conclude that these events are probably type III bursts (Kai, Melrose, & Suzuki 1985). The brightness temperatures of the bursts may be underestimated due to (1) the 10 s time averaging that was used and (2) scattering of the radio emission by coronal turbulence, which broadens the angular size of the sources (Bastian 1994).

In contrast to the 400 cm sources, the 91.6 cm emission is contained within a more compact (angular size $\theta \approx 1.5$), stationary (to within $30''$), and more symmetrical source that lies at a lower projected height of $h \approx 0.15$ $R_\odot$ above the limb. Impulsive bursts with durations as short as 10 s and brightness temperatures of $T_b = 2$–$3.8 \times 10^6$ K are superposed on a more slowly varying (hours) and increasingly intense continuum level that only became detectable at 19:40 UT. Unlike the 400 cm bursts, the 91 cm bursts were cospatial with the continuum source to within $10''$.

Both the bursts and continuum at 91 cm are nearly 100% right-circularly polarized, which suggests that the emission is nonthermal and can most probably be identified as a type I noise storm. If this is the case, then we would expect that the right-circularly polarized 91 cm source to be emitted in the *o*-mode of wave propagation and that the magnetic structure containing the noise storm connects to a region of negative polarity in the photosphere (see Kai et al. 1985). Examination of Kitt Peak magnetograms showed that the dominant sunspot in the nearest active region, AR 8176 (S43°, E66°), did, in fact, have negative polarity, which supports the idea that the 91 cm emission observed on March 8 is a type I noise storm located on large-scale magnetic loops linked to AR 8176.

As can be seen in Figures 1 and 2, the 400 and 91 cm sources do not lie directly above either of the active regions—AR 8175 (N44°, E56°) and AR 8176 (S43°, E66°)—detected near the limb on the EIT spectroheliograms but instead appear to lie in the corona between these regions. If the impulsive 400 cm radiation is due to type III burst activity and the 91 cm radiation to type I noise storm emission, both at the fundamental of the plasma frequency, then we infer respective electron densities of $N_e \approx 0.6 \times 10^8$ and $\approx 1.2 \times 10^9$ cm$^{-3}$ at the heights of these sources. Successive nonthermal bursts at 400 cm appear to form at about the same radial distance but at different locations along an otherwise invisible, large-scale loop, perhaps linked to the active regions AR 8175 and AR 8176 and/or to an active region behind the east limb. The EIT images taken in the lines of He II ($8 \times 10^4$ K; 304 Å), Fe IX/X ($1.0 \times 10^6$ K; 171 Å), and
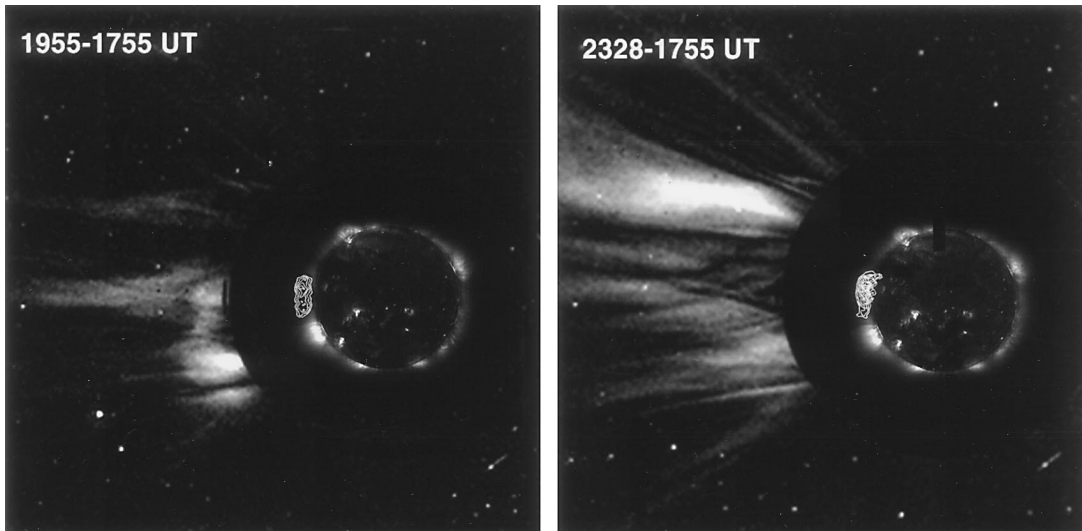
FIG. 3.—*SOHO* LASCO C2 coronagraph images, compared with EIT Fe XII (195 Å) images and VLA 400 cm maps. The LASCO image on the left, formed from the difference of images taken at the UT times in the upper left-hand corner, shows a coronal mass ejection whose outward motion was estimated from successive difference images at a velocity of 305 km s$^{-1}$. It probably coincided with a disk event occurring at 19:14 UT, the time of the VLA and EIT images. The LASCO difference images on the right, also taken from times denoted in the upper left-hand corner, is compared with VLA and EIT data taken at 22:21 UT.

Fe XV ($2.0 \times 10^6$ K; 284 Å) on March 8 and over the next several days showed no evidence for large-scale coronal features that might be candidates for such a loop, which suggests that any hot plasma constrained within the large-scale magnetic loops has a relatively low emission measure.

Examination of the *SOHO* full-disk EIT 195 Å images revealed that AR 8176 produced transient extreme-ultraviolet (EUV) brightenings starting at 19:14:12 UT (see arrow in Fig. 1) and continuing until 20:38:15 UT. The initial activity was probably associated with a C1.1 GOES X-ray burst that began at 19:02 UT and reached a maximum at 19:24 UT (Solar-Geophysical Data Prompt Report). The EUV and soft X-ray events were then followed by a coronal mass ejection detected by the Mauna Loa Mark III K coronagraph at a position angle of 110° between 19:14 and 1958 UT and by the LASCO C2 coronagraph at 19:55 UT. This event was described in the Mauna Loa Solar Observatory (MLSO) archives as a classic advancing loop followed by embedded prominence material. Construction of a height-time plot using Mauna Loa images that could detect structures between 1.12 and 2.44 $R_\odot$ yields a speed of $v \approx 305$ km s$^{-1}$ for the CME. Extrapolating to the solar surface yields a CME onset time of 18:56 UT, but this is probably a lower limit because the CME very likely did not originate in the photosphere. For example, the faint white-light emission that could be recognized as the CME was first detected at 19:14 UT by the MLSO coronagraph at a radial distance of $r \approx 1.73$ $R_\odot$, which suggests that the CME originated somewhere in the low corona rather than at the solar surface.

In Figure 3 we compare VLA and EIT images with difference images taken by the LASCO C2 coronagraph showing the location of this CME as well as a spatially separate ejected component detected above the northeast limb at position angle ≈65°. This figure shows that the trajectory of the initial CME extends radially outward from AR 8176 while the subsequent ejection, which was first detected by LASCO at 23:28 UT, appears to extend outward from AR 8175 in the northeast. In neither case does the 400 cm source lie along the trajectories of the CMEs, but it instead lies between them. The nonthermal metric bursts at 400 cm may be related to a single long-duration (hours)

CME transient with spatially separate components or to two CMEs near the beginning and end of this time interval.

## 3. DISCUSSION

Our VLA observations have spatially resolved both impulsive and long-lasting components of the 400 cm burst emission and have shown that they lie in the low corona between active regions, possibly along large-scale magnetic loops that are otherwise invisible at EUV and soft X-ray wavelengths. The fact that these nonthermal radio bursts increase in intensity and appear sporadically several hours after the initial episode of energy release suggests that the emitting nonthermal particles can be stored and reaccelerated in the corona. No 400 cm bursts or 91 cm noise storm enhancements were detected during the hour preceding the CME activity, which suggests that the nonthermal radio bursts were associated with CME activity. This conclusion is also supported by the similar spatial location of the CMEs and long-wavelength (400 and 91 cm) radio emission.

The radiation mechanism of the longer lasting, low-brightness 400 cm continuum sources, which are spatially separated by a few arcminutes from the 400 cm bursts, is unknown, although they might represent relatively compact regions of thermal emission similar to that detected by the now-defunct Culgoora and Clark Lake radioheliographs at meter wavelengths (e.g., Sheridan et al. 1978; Kundu & Gopalswamy 1990; Gopalswamy & Kundu 1992, 1993). If thermal bremsstrahlung is assumed, then using a peak brightness temperature of $T_b \approx 6 \times 10^5$ K and a coronal electron temperature of $T_e = 2 \times 10^6$ K, we derive an optical depth of $\tau_{TB} \approx 0.3$ at 74 MHz. For a source thickness $L$ of $1.1 \times 10^{10}$ cm, which corresponds to the approximate source angular size of 2′.5 at half intensity, we derive an electron density of $N_e \approx 1.1 \times 10^7$ cm$^{-3}$. The fact that the brightness temperature of the quiescent emission does not detectably vary with time suggests that the density or temperature of the thermal plasma in this region also remains relatively constant.

The fact that the 91 cm noise storm appears to have been

initiated soon after the start of the first CME is a particularly interesting result and suggests some sort of physical relationship between the production of nonthermal particles and changes in the coronal plasma–magnetic field structure. Perturbations in the local plasma density, as well as the reorganization of large-scale magnetic fields, might be created by the passage of a nearby CME, leading to the onset of nonthermal energy release in the form of type I noise storms and type III bursts. A comparison of radio noise storms and *Solar Maximum Mission* coronagraph observations has previously indicated that nonthermal noise storm enhancements are correlated with the addition of coronal material in their vicinity, either by CMEs or by other visible brightenings (Kerdraon et al. 1983). More recently, VLA observations at 91 cm indicate that noise storm emission was associated with large-scale magnetic structures in which a coronal mass ejection eventually occurred (Habbal et al. 1996). The onsets of two CMEs detected with the LASCO C2 and C3 coronagraphs have also been associated with the enhancement of preexisting nonthermal radio noise storms (Aurass et al. 1997).

## 4. CONCLUSIONS

We have demonstrated that the VLA can image meter wavelength (400 cm) nonthermal bursts and possibly thermal emission associated with CMEs with extraordinary spatial (30″) and temporal (10 s) resolution. Related nonthermal emission is also detected with the VLA at 91 cm wavelength with similar spatial (7″) and temporal (1.7 s) resolution. Both the 400 cm bursts and 91 cm noise storm enhancements continued for a period of 3 hr, providing evidence for long-lasting nonthermal particle acceleration associated with CMEs. The rough spatial and temporal coincidence between the initial CME activity and the nonthermal burst activity strongly suggests that energetic radio-emitting particles are accelerated during the CME event and long after it. The location of the 400 cm bursts and continuum in extended sources between and above two active regions suggests that the particle acceleration occurs in large-scale interacting magnetic structures that connect active regions to more distant active regions on the Sun. Such interactions leading to magnetic reconnection and long-duration meter wavelength radio emission have also been inferred from simultaneous LASCO and Nancay radioheliograph observations (Maia et al. 1998; Pick et al. 1997, 1998).

## REFERENCES

Aurass, H., Mann, G., Ryer, M., Andrews, M. D., Michels, D. J., Paswaters, S. E., & Tappin, S. J. 1997, in Proc. Fifth *SOHO* Workshop: The Corona and Solar Winds Near Minimum Activity (ESA SP-404; Noordwijk: ESA), 183
Bastian, T. S. 1994, ApJ, 426, 774
Bogod, V. M., Garimov, V., Gelfreikh, G. B., Lang, K. R., Willson, R. F., & Kile, J. N. 1995, Sol. Phys., 160, 133
Erickson, W. C. 1984, J. Astrophys. Astr., 5, 55
Gopalswamy, N., & Kundu, M. R. 1992, ApJ, 390, L38
———. 1993, Sol. Phys., 143, 327
Habbal, S. R., Mossman, A., Gonzalez, R., & Esser, R. 1996, J. Geophys. Res., 101, 19,943
Kai, K., Melrose, D. B., & Suzuki, S. 1985, in Solar Radiophysics, ed. D. J. McClean & N. K. Labrum (New York: Cambridge Univ. Press), 413
Kerdraon, A., Pick, M., Trottet, G., Sawyer, C., Illing, R., Wagner, W., & House, L. 1983, ApJ, 265, L19
Krucker, S., Benz, A. O., Aschwanden, M. J., & Bastian, T. S. 1995, Sol. Phys., 160, 151

Kundu, M. R., & Gopalswamy, N. 1990, Sol. Phys., 129, 133
Maia, D., et al. 1998, Sol. Phys., in press
Pick, M., Maia, D., Howard, R., Kerdraon, A., Brueckner, G. E., Lamy, P., Schwenn, R., & Aurass, H. 1997, in the Proc. Fifth *SOHO* Workshop: The Corona and Solar Wind Near Minimum Activity (ESA SP-404; Noordwijk: ESA), 601
Pick, M., et al. 1998, Sol. Phys., in press
Sheridan, K. V., Jackson, B. V., McClean, D. J., & Dulk, G. A. 1978, Proc. Astron. Soc. Australia, 3, 249
Stewart, R. T., & McLean, D. J. 1982, Proc. Astron. Soc. Australia, 4, 386
Trottet, G., Pick, M., House, L., Illing, R., Sawyer, C., & Wagner, W. 1982, A&A, 111, 306
Wagner, W. J. 1984, ARA&A, 22, 267
White, S. M., Thejappa, G., & Kundu, M. R. 1992, Sol. Phys., 138, 163
Willson, R. F., Kile, J. N., Donaldson, S. R., Lang, K. R., Gelfreikh, G. B., & Bogod, V. M. 1995, Adv. Space Res., 17, 265
Willson, R. F., Kile, J. N., & Rothberg, B. 1997, Sol. Phys., 170, 299